nature physics

ARTICLES

PUBLISHED ONLINE: 21 AUGUST 2011 | DOI: 10.1038/NPHYS2063

Robust optical delay lines with topological protection

Mohammad Hafezi[1]*, Eugene A. Demler[2], Mikhail D. Lukin[2] and Jacob M. Taylor[1]

Phenomena associated with the topological properties of physical systems can be naturally robust against perturbations. This robustness is exemplified by quantized conductance and edge state transport in the quantum Hall and quantum spin Hall effects. Here we show how exploiting topological properties of optical systems can be used to improve photonic devices. We demonstrate how quantum spin Hall Hamiltonians can be created with linear optical elements using a network of coupled resonator optical waveguides (CROW) in two dimensions. We find that key features of quantum Hall systems, including the characteristic Hofstadter butterfly and robust edge state transport, can be obtained in such systems. As a specific application, we show that topological protection can be used to improve the performance of optical delay lines and to overcome some limitations related to disorder in photonic technologies.

Particles in two-dimensional structures with a magnetic field exhibit a remarkable variety of macroscopic quantum phenomena, including integer[1] and fractional[2] quantum Hall and quantum spin Hall effects[3], and predicted regimes of fractional or non-Abelian statistics[4,5]. A hallmark of these systems is the presence of edge states, with transport properties that are robust against disorder and scattering, leading to a quantized conductance sufficient to provide a resistance standard[6,7]. The natural robustness of topological states is actively explored in quantum computation to achieve fault-tolerant operations[8,9]. Recently, approaches to observing similar quantum Hall behaviour in bosonic systems, including ultra-cold gases (for a review see ref. 10) and photons[11–16], have been suggested. In particular, simulation of the Hofstadter butterfly spectrum using the one-dimensional Harper equation[17,18] was suggested in ref. 19.

Our method for realization of topological protected photonic devices focuses on two-dimensional arrays of coupled resonator optical waveguides (CROW) with appropriate linear optical devices. We can simulate a 2D magnetic tight-binding Hamiltonian with degenerate clockwise and counter-clockwise modes. This approach does not require explicit time-reversal symmetry breaking[11–15], but the degenerate modes—time-reversed pairs—behave analogously to spins with spin–orbit coupling in the electronic quantum spin Hall effect (QSHE; refs 20–22), and experience a spin-dependent magnetic field (Fig. 1). When the clockwise and counter-clockwise modes are decoupled, we can selectively drive each mode and observe quantum Hall behaviours without breaking the time-reversal symmetry in the tight-binding Hamiltonian. In a direct analogy to the electronic integer quantum Hall effect, we show that photonic edge states carry light at the perimeter of the system, while being insensitive to disorder, and therefore form a basis for robust photonic devices. In particular, in comparison to state-of-the-art 1D CROW systems[23,24], our approach can be more resistant to scattering disorders and fabrication errors.

2D photonic system and quantum spin Hall Hamiltonian

As illustrated in Fig. 1, our system comprises optical ring microresonators that support degenerate clockwise and counter-clockwise modes, restricted to one pair per resonator. We consider these modes as two components of a pseudo-spin, that is, clockwise ($\sigma=-1$, or psuedo-spin down) and counter-clockwise ($\sigma=+1$, pseudo-spin up) circulation. Resonators—evanescently coupled to each other—have been studied in the context of 1D CROW (ref. 25), where the coupling leads to a tight-binding model for photons and the corresponding photonic band structure. By coupling these modes in a two-dimensional arrangement, as we show below under appropriate conditions, the dynamics of such a photonic system is described by a Hamiltonian for charged bosons on a square lattice (tight-binding), but with the addition of a perpendicular, pseudo-spin-dependent effective magnetic field:

$$H_0 = -\kappa\left(\sum_{\sigma,x,y}\hat{a}^{\dagger}_{\sigma x+1,y}\hat{a}_{\sigma x,y}e^{-i2\pi\alpha y\sigma}+\hat{a}^{\dagger}_{\sigma x,y}\hat{a}_{\sigma x+1,y}e^{i2\pi\alpha y\sigma} + \hat{a}^{\dagger}_{\sigma x,y+1}\hat{a}_{\sigma x,y}+\hat{a}^{\dagger}_{\sigma x,y}\hat{a}_{\sigma x,y+1}\right) \quad (1)$$

where κ is the coupling rate of optical modes and $\hat{a}^{\dagger}_{\sigma x,y}$ is the photon creation operator at the resonator at site (x,y) with different pseudo-spin components, $\sigma=\pm1$. Specifically, photons acquire a $2\pi\alpha\sigma$ phase when they go around a plaquette—equivalent to having α quanta of magnetic flux penetrating each plaquette[26,27].

To derive the Hamiltonian description, we start by considering two coupled resonators (Fig. 1a), focusing only on the counter-clockwise modes inside each resonator. The length of connecting waveguides is chosen such that photons respectively destructively (constructively) interfere inside the waveguide loop (resonator) and, therefore, they will be confined in the resonators rather than waveguides. Moreover, the lengths of the upper and lower branches of the waveguide differ from each other, so when a photon hops from the left to the right resonator it acquires a different phase from that when it hops in the opposite direction. This can be formally verified using the standard input–output formalism[28]. In particular, the boundary condition at the left resonator can be written as

$$\hat{E}^{\mathrm{out}}_x=\hat{E}^{\mathrm{in}}_x+\sqrt{2\kappa}\hat{a}_x$$

where the $\hat{E}_x$ are waveguide electric field operators in the vicinity of the xth resonator and $\hat{a}_x$ is the resonator electric field operator, as shown in Fig. 1a. The resonator field equation of motion is $\partial_t\hat{a}_x=$

[1]Joint Quantum Institute, University of Maryland and NIST, College Park, Maryland 20742, USA, [2]Physics Department, Harvard University, Cambridge, Massachusetts 02138, USA. *e-mail: hafezi@umd.edu.

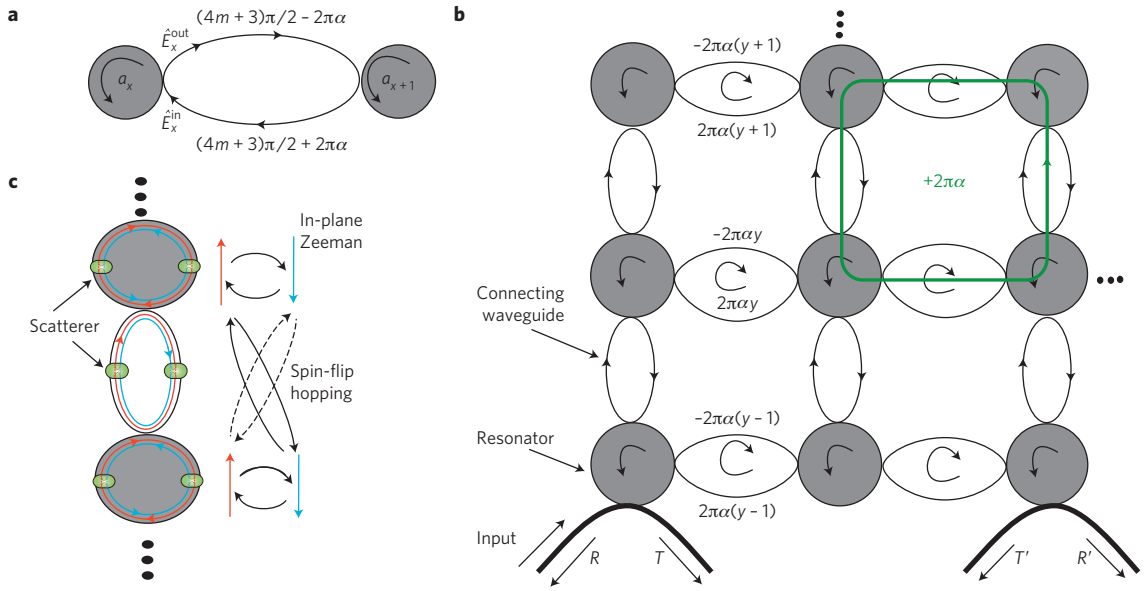

Figure 1 | Schematics of the photonic system with a synthetic magnetic field. a, The dynamics of two coupled resonators is governed by a magnetic-type Hamiltonian (equation (2)). The lengths of the upper and lower branch differ from each other such that the phase difference is $4\pi\alpha$ and m is an integer. **b**, A magnetic tight-binding model can be implemented in a 2D lattice of coupled resonators. Only the waveguide phase differences are shown. **c**, By introducing scatterers in resonators and waveguides, one can induce in-plane magnetic field (Zeeman) and spin-flip hopping terms, in analogy to quantum spin Hall models.

$-\kappa\hat{a}_x - \sqrt{2\kappa}\hat{E}_x^{in}$, and similarly for the right resonator. Photons propagate freely between the resonators, so for the upper branch we have $E_{x+1}^{in} = -iE_x^{out}\exp(-2\pi i\alpha)$, and similarly for the lower branch. By eliminating the waveguide fields, the left and right resonator field dynamics will be given by $\partial_t\hat{a}_{x(x+1)} = i\kappa\exp(\pm 2\pi i\alpha)\hat{a}_{x+1(x)}$, consistent with photon tunnelling between the resonators. The corresponding Hamiltonian of the two resonators takes the form:

$$H_{two-res} = -\kappa\hat{a}_{x+1}^{\dagger}\hat{a}_x e^{-2\pi i\alpha} - \kappa\hat{a}_x^{\dagger}\hat{a}_{x+1}e^{2\pi i\alpha} \qquad (2)$$

The above analysis for counter-clockwise modes (pseudo-spin up $\hat{a}_{\uparrow x,y}$) in the resonators shows that, in the absence of backscattering, they are decoupled from their time-reversed counterpart, that is, the clockwise mode of the resonator (pseudo-spin down $\hat{a}_{\downarrow x,y}$). At the same time, the pseudo-spin down component will experience a magnetic field similar to the pseudo-spin up component, where only the sign of magnetic field is changed ($\alpha \to -\alpha$). Now, by connecting resonators in a lattice structure and tuning the phase of the connecting waveguides, we can arrange the acquired phase around each plaquette to be uniform and equal to $2\pi\alpha$. The phase can be tuned either by changing the length (or the index of refraction) of the connecting waveguides or by coupling ring resonators to the sides of the waveguides (similar to a Mach–Zehnder configuration[29,30]). The implementation of a Landau-type gauge is shown in Fig. 1b, where the corresponding Hamiltonian is the form of equation (1). Indeed, this is the trivial form of QSHE Hamiltonians in an analogy to time-reversal invariant spin–orbit interactions in solid state systems[20–22], where the gauge field has opposite orientations for the two pseudo-spin components.

Generalized pseudo-spin–orbit interaction

Furthermore, one can control the coupling between different pseudo-spin component and exploit a wider class of QSHE Hamiltonians on a square lattice. In particular, semi-transparent scatterers inside the resonators or the connecting waveguides can be engineered to mix different pseudo-spin components with each other.

To illustrate this mixing, we consider the addition of a pair of scatterers in every vertical connecting waveguide, as shown in Fig. 1c. For simplicity, we assume the scattering is weak and does not introduce any loss. We characterize the strength of the scatterer by a parameter ϵ, where the transmission coefficient is near unity ($t_s \simeq 1$) and the reflection coefficient is $r_s = i\epsilon/\sqrt{2}$. As shown in the Supplementary Information, the corresponding Hamiltonian of a single vertical array of resonators will be:

$$H_{flip} = -\kappa\sum_{x,y}\begin{pmatrix}\hat{a}_{\uparrow x,y+1}^{\dagger} & \hat{a}_{\downarrow x,y+1}^{\dagger}\end{pmatrix}\begin{pmatrix}1 & \epsilon\\ \epsilon & 1\end{pmatrix}\begin{pmatrix}\hat{a}_{\uparrow x,y}\\ \hat{a}_{\downarrow x,y}\end{pmatrix} + \text{h.c.}$$

The diagonal terms are identical to the tight-binding terms of equation (1) and the off-diagonal terms represent hopping between two adjacent sites while undergoing a spin-flip, that is, the scatterers couple clockwise to counter-clockwise photons (Fig. 1c). This spin-flip hopping is similar to the Rashba term in the context of spin–orbit interaction[21,31].

Similarly, if we consider a pair of weak scatterers inside the resonators, then corresponding Hamiltonian takes the form:

$$H_{mag} = -\kappa\sum_{x,,y}\begin{pmatrix}\hat{a}_{\uparrow x,y+1}^{\dagger} & \hat{a}_{\downarrow x,y+1}^{\dagger}\end{pmatrix}\begin{pmatrix}1 & 0\\ 0 & 1\end{pmatrix}\begin{pmatrix}\hat{a}_{\uparrow x,y}\\ \hat{a}_{\downarrow x,y}\end{pmatrix} + \text{h.c.}$$
$$-\frac{4\epsilon\kappa\mathcal{F}}{\pi}\sum_{x,y}\begin{pmatrix}\hat{a}_{\uparrow x,y}^{\dagger} & \hat{a}_{\downarrow x,y}^{\dagger}\end{pmatrix}\begin{pmatrix}0 & 1\\ 1 & 0\end{pmatrix}\begin{pmatrix}\hat{a}_{\uparrow x,y}\\ \hat{a}_{\downarrow x,y}\end{pmatrix}$$

The first term is the usual tight-binding form and the second term represents the in-plane magnetic field, which is enhanced by the finesse of the resonators (that is, number of photon round trips $\mathcal{F} \simeq \pi/(1-r^2)$). If these vertical arrays replace the vertical arrays of Fig. 1b, then the overall Hamiltonian of the system encompasses both an in-plane Zeeman term (due to on-site scattering) and a hopping spin-flip term (similar to the Rashba interaction).

Probing the photonic system

We now show how optical spectroscopy measurements can be harnessed to analyse the transport properties of our photonic system. As shown diagrammatically in Fig. 1b, we can evaluate the transmission and the reflection of an input light field by coupling two probe waveguides to the lattice edges. The magnetic states

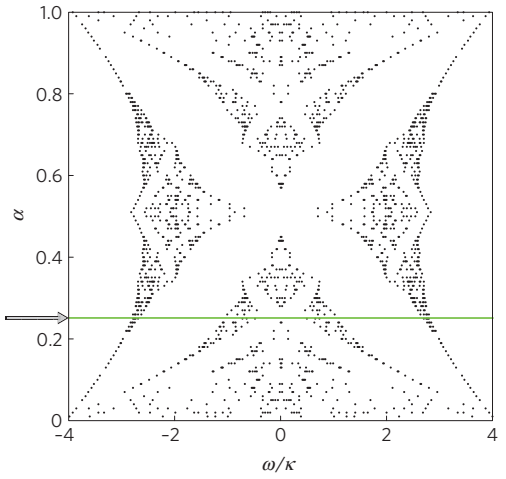

Figure 2 | Hofstadter butterfly spectrum. Each point represents a reflectivity greater than 0.005, for a 10×10 lattice with torus boundary condition and coupling $\nu/\kappa = 0.02$. The green line is a guide for the eye to show the spectrum at the magnetic field of interest (α) for the remaining figures in the article.

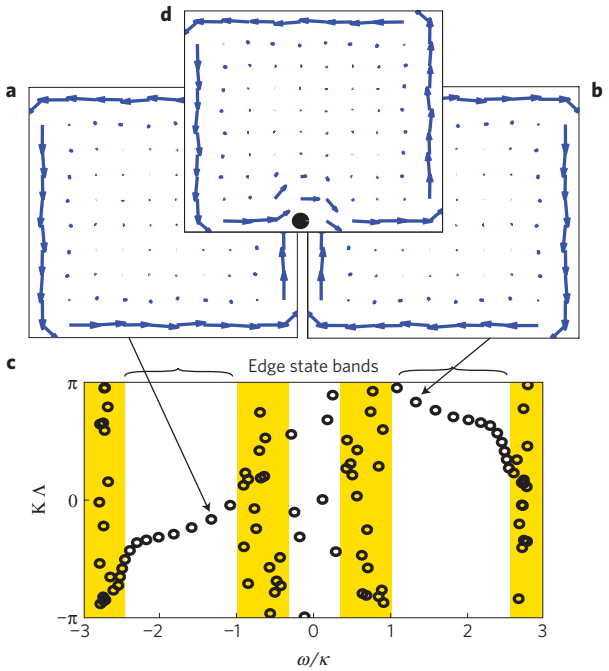

Figure 3 | Edge states and their dispersion. Light intensity for a forward-going (**a**) edge state in the absence of disorder and its backward-going counterpart (**b**). **c**, Shows the dispersion relation; a wave number is evaluated for each energy eigenstate at the lower edge, that is, KΛ is the phase difference between two consecutive resonators at the edges. Magnetic band states do not have a uniform phase difference along the edges and are shown in the yellow area. The arrows show the states corresponding to **a** and **b**. **d** Shows the light intensity routes around the disorder (black dot, $U/\kappa = 20$). In these plots, a 10×10 square lattice with $\alpha = 1/4$ is considered.

of the system (bulk states and edge states) will manifest in such transmission spectroscopy.

Consider the simplest case of the quantum spin Hall effect, where pseudo-spin-flip terms are absent. In this regime, we have two decoupled copies of regular quantum Hall states, one for each pseudo-spin component. In the rest of the article, we restrict our analysis to a single spin component, and for brevity, we drop the spin index. This choice enables us to examine in detail methods for probing the system and determining its response to disorder.

Using a formalism similar to quantum scattering theory, we investigate the problem of scattering of light fields in optical waveguides connected to our photonic system and evaluate the transmission and reflection coefficients under various conditions. The waveguides only couple to co-propagating modes in the resonators (counter-clockwise in Fig. 1b), and thus under our assumption, the reflection in the input channel and transmission in the output channel are zero (that is, $R, T' = 0$ as shown in Fig. 1b). The input–output probing waveguides are coupled to two resonators in the systems, denoted by $|\mathrm{in}\rangle$ and $|\mathrm{out}\rangle$, respectively. As shown in the Supplementary Information, the self-energy of these resonators can be written as $\Sigma = -i(\nu/2)|\mathrm{in}\rangle\langle\mathrm{in}| - i(\nu/2)|\mathrm{out}\rangle\langle\mathrm{out}|$, where the coupling strength is defined as ν. Using the Lippman–Schwinger equation, one can deduce different reflection/transmission coefficients[32,33]. In particular, the reflection coefficient is given by

$$r'(\omega) = -i\nu\left\langle \mathrm{out}\left|\frac{1}{\omega - H_0 - \Sigma}\right|\mathrm{in}\right\rangle \qquad (3)$$

where ω is the detuning from the resonators. Thus, appreciable reflection should be observed when the frequency of an incoming photon becomes resonant with the energy of a photonic state inside the system. Note that if the photonic system is a single resonator, equation (3) reduces to the familiar form: $r'(\omega) = \nu/(i\omega - \nu)$.

The energy spectrum of the H_0 for an infinite lattice is the well-known Hofstadter butterfly[27]. We consider a $N_x \times N_y$ lattice with torus boundary condition (that is, coupling top–bottom and left–right edges together) to simulate the effect of an infinite lattice. According to the Hofstadter spectrum, for rational magnetic fluxes ($\alpha = p/q$), each magnetic band has many states ($N_x N_y/q$), which is reminiscent of Landau level degeneracy in the continuum. The result of our numerical solution is shown in Fig. 2, where the reflectivity ($R' = |r'(\omega)|^2$) is evaluated for different frequencies and magnetic field (α) by the formalism described above. High reflectivity occurs when the lower waveguide light is coupled to the system and completely transferred to the reflection output channel (the second waveguide), similar to a channel drop filter. We can readily see that the energy spectrum of the uncoupled system (Hofstadter butterfly) can be obtained by measuring the system reflectivity. We note that to resolve different energy levels in the spectrum, the probe waveguide coupling (ν) should be chosen to be sufficiently narrow ($\lesssim 8\kappa/(N_x N_y)$).

Photonic edge states

In contrast to toroidal boundary conditions, where only magnetic bands are present, in a finite square lattice there exist states between magnetic bands which are known as 'edge states'. A direct analogy to 2D electrons in a magnetic field (quantum Hall physics)[34–36] suggests there should be quasi-one dimensional states localized at the perimeter of the system which carry current and are immune to disorders in the form of random potential. In particular, for certain bands, the field in resonators located in the bulk (away from the edges) undergoes destructive interference and, therefore, the light intensity (that is, the current probability of $\hat{a}_{x,y}$) is non-zero only at the edges. This is illustrated in Fig. 3a. For each edge state, there is a corresponding edge state with an opposite chirality (Fig. 3b). More specifically, the forward- and backward-propagating edge states take different paths and, consequently, they have different resonances at detuning, equal in magnitude and opposite in sign. This is similar to the behaviour of an electron with a non-zero orbital angular momentum which can be aligned or anti-aligned with an external magnetic field. For edge states, the phase difference between two consecutive resonators is uniform along the edges

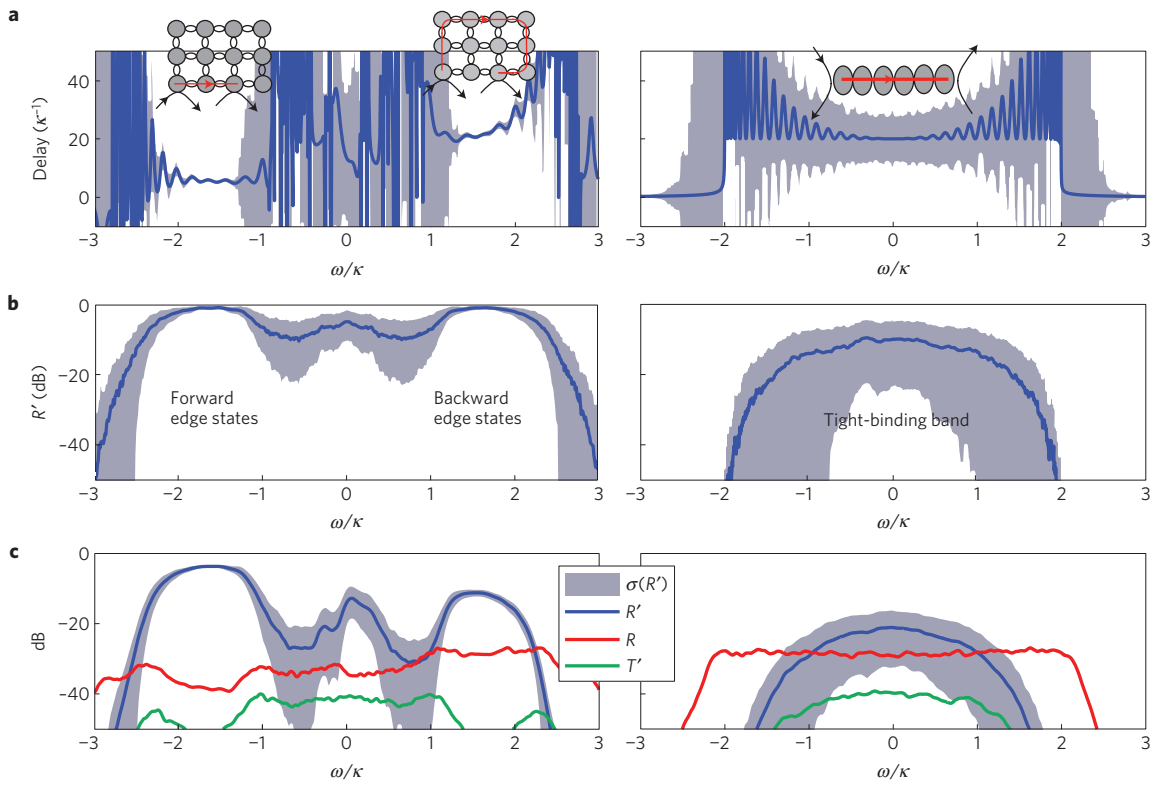

Figure 4 | Edge states versus CROW. This figure compares the quantum Hall system (left panels, 10×10 lattice) and CROW (right panels, array of 40) performances as delay lines. In **a** and **b** blue curves show the average time delay and output reflectivity, respectively, and the grey area highlights the standard deviations in the presence of non-magnetic disorder (a Gaussian disorder with $\sigma(U)/\kappa = 0.4$ for 500 realizations). Whereas the transport is quite noisy in the magnetic bands and CROW (tight-binding band), the edge-state bands exhibit noiseless transport with delays comparable to CROW. Depending on the input frequency, different edge states participate in the transport, which leads to shorter or longer delays, as shown in the insets. **c,** Magnetic disorder: besides the non-magnetic disorder, to estimate the effect of magnetic disorder and loss, a Gaussian distribution of magnetic noise (mode coupling) with a width $\epsilon\mathcal{F} = 0.1$, a random phase ($[0, 2\pi)$) and an intrinsic loss ($\kappa_{\text{in}} = 0.02\kappa$), is assigned to each resonator. We observe that the transport properties are more degraded for CROW than edge-state bands. Whereas the counter-clockwise modes of the resonators are excited through an input field, the onsite scatterers backscatter photons in the clockwise modes. These modes leak out into R and T' channels, which are non-zero in these plots. The coupling between input and output waveguides and the system is chosen to optimize the transport (for edge states $v = 6\kappa$ and for CROW $v = 2\kappa$). In the quantum Hall system, the input and output waveguides are coupled to $(x = 2, y = 1)$ and $(x = N_x - 1, y = 1)$ resonators, respectively.

(that is, well-defined momentum) and the system has a smooth dispersion (that is, the phase difference is a smooth function of frequency) only in the edge state bands, as shown in Fig. 3c.

To illustrate the robustness of the system to disorder, we consider that each resonator may be detuned from its neighbours. This provides a model for 'non-magnetic' disorder characterized by a random on-site potential at each site ($U_{x,y}\hat{a}^{\dagger}_{x,y}\hat{a}_{x,y}$). Such imperfections are a common problem in photonics and prevent coupling large numbers of resonators[23,37,38].

In electronic quantum Hall systems the edge states are immune to disorder[5]. We find that such robustness applies to our photonics system. When disorder is located in the bulk, the edge state is obviously not affected. However, when disorder is located on the edge, the edge state routes around it, as shown in Fig. 3d for the test case of a single disordered site. More precisely, scattering which would reverse the current is prevented because the backward going edge state has a different energy, as discussed above, preventing elastic scattering.

Application to delay lines

Transport through edge states requires the photon to traverse the perimeter of the system, leading to a sizeable time delay. We now examine how our system provides a robust alternative to conventional CROW in photonic delay lines. For illustration, we compare the transport properties of our photonic quantum Hall (QH) system to a conventional 1D CROW system, as shown in Fig. 4. In the quantum Hall system, there is a robust transfer band provided by edge states that carry photons from the input waveguide to the output waveguide (Fig. 4 inset), in a direct analogy to electronic edge states in the context of the integer quantum Hall effect[34].

We first consider both systems without disorder to find their operational bandwidth and delay time in transport. In both cases, the operational bandwidth is given by the smooth, linear part of the dispersion relation. In the quantum Hall system, the edge state band (Fig. 3c) is located between two Hofstadter bands (Fig. 2), whereas in the CROW configuration, the operational bandwidth is in the middle of the tight-binding dispersion to avoid the group velocity dispersion[25]. Moreover, in both systems, the delay time is proportional to the number of resonators involved in the transport ($\tau \simeq (\kappa/2)N$), as shown in Fig. 5a. In the quantum Hall system, the transport can be either performed along the long or short edge of the system, depending on the input frequency, as shown schematically in the inset of Fig. 4. In both systems, in the absence of disorder, the bandwidth-delay product increases with the length/perimeter of the system.

However, in the presence of disorder, CROW and edge states behave differently as the system size increases. In particular, in 1D systems (for example CROW) the disorder leads to localization[39,40] and, therefore, the transmission is impeded. More specifically, one finds a localization length $l \simeq 10\kappa^2/\text{var}(U)$, where $\text{var}(U)$ is the

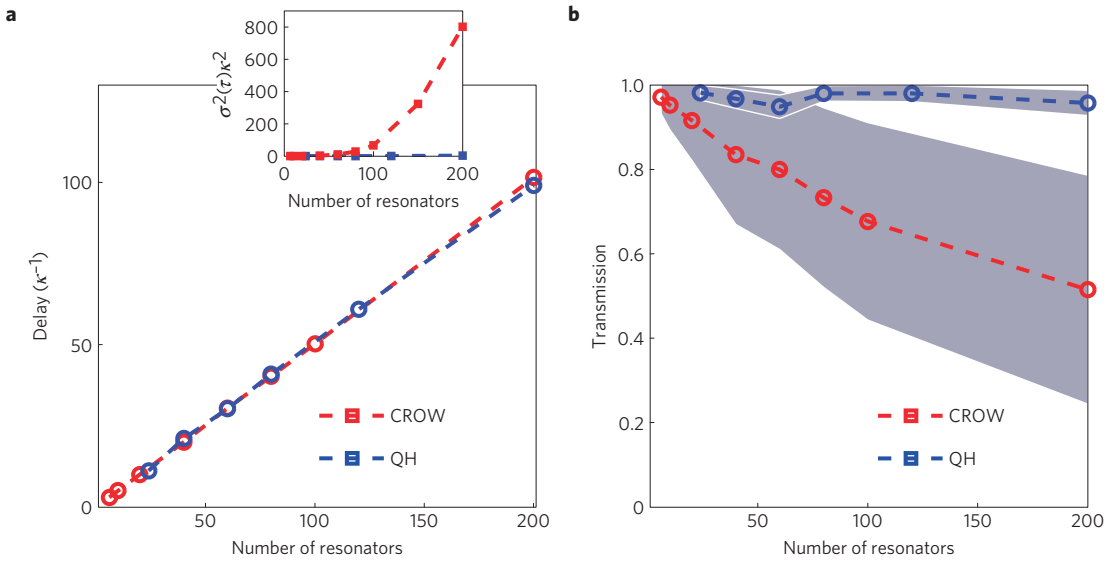

Figure 5 | 1D localization versus robust edge states. For 1D CROW and 2D quantum Hall, the transport properties are evaluated at the centre frequency $\omega = 0$ and $\omega = 1.5\kappa$ respectively, where the group velocity dispersion is minimum. Gaussian disorder is assumed with $\sigma(U)/\kappa = 0.14$ and the transmission is averaged over an ensemble of 1,000 realizations. **a**, Compares time delay. **b**, Compares transmission (R'). On increasing the system length/perimeter (x axis), the transmission for 1D CROW decreases and the noise (standard deviation in grey) increases[24], whereas both the transmission and the noise in the 2D quantum Hall system remains constant. The inset shows the standard deviation of the time delay in both systems for **a**. To highlight the effect of localization, the loss is ignored in these plots.

variance of the disorder[40]; when $N_x > l$, all states are localized[41,42], whereas for $N_x < l$ the transmission is drastically perturbed and 'ripples' appear in the transmission spectrum[23,38] and the delay time spectrum[24]. Decreasing the resonator quality factor effectively increases the localization length and postpones the localization effects; nevertheless, the noise in the time delay increases with the number of resonators[24]. Physically the forward- and backward-going states have the same energy and spatially overlap, and, therefore, they easily scatter from each other. In contrast, in our 2D quantum Hall system, the forward- and backward-going edge state have different energies and are topologically protected against disorder[5,36,43]. To confirm that our edge states provide a robust transport, we numerically study the effect of disorder, by assigning a random frequency mismatch to each resonator and taking the average over many 'frozen' disorder realizations (see ref. 44 for transverse localization). By studying the transmission at the 'sweet' frequency ($\omega = 0$ for 1D CROW and the middle of edge state band ($\omega = 1.5\kappa$) for QH), we observe that by increasing the system length/perimeter the transmission in CROW decreases whereas the transmission through edge states is unaffected, as shown in Fig. 5b. Similarly the delay changes significantly from system to system in 1D CROW; single disorder realization exhibits ripples in the transmission and delay time spectrum (as shown in Supplementary Information). To characterize this behaviour, we evaluate the standard deviation for each frequency and observe that whereas the 'time delay ripples' increases in 1D CROW (ref. 24), the QH system shows an almost complete absence of such ripples (see Methods).

Outlook

Optical signals might be a promising alternative to electronic signals in future circuits. A key requirement is the ability to filter and slow down light on-chip over a large bandwidth (several Gbps) for various time-domain processing applications, such as optical buffering and multiplexing[45]. However, the effect of disorder in the millimetre-size footprint is detrimental, for example, 'ripples' in the transmission spectrum[23,38] and noise in the delay time[24], which increases with the number of resonators. Our system provides a platform to realize a photonic system robust against disorder.

In addition, our photonic system enables a new approach for exploration of various fundamental quantum Hall phenomena. This photonic system not only enables investigations of quantum Hall physics by simulating different types of Hamiltonian at room temperature, but it also taps into topological features to provide new devices for photonics. In the non-interacting regime (which was the topic of this article), one can explore the Hofstadter butterfly of photons and photonic edge states as delay lines immune to disorders and also localization in 2D for non-interacting particles[44,46]. Furthermore, with the addition of interaction between photons[44,47,48], this system opens up exciting prospects for exploring many-body, topological states of light. Although the ground state properties of such systems have been extensively studied, the suitable characterization and measurement of strongly interacting photons is still an open question. In particular, chemical energy is absent for photons, and the relevant conditions to study photons involves an externally driven system, which naturally leads to non-equilibrium steady states[49]. Another advantage of photons is their flexibility to form various system topologies (tori with different genera) by simply connecting waveguides to each other and manipulating such states for topological quantum computation. Intriguing additional applications of these ideas await further exploration.

Methods

For simulation, we have considered a square lattice for the QH system, but any other shape with the same topology (for example rectangle) behaves similarly, as the topological nature dictates. We have compared both systems for a fixed system size and studied the transport spectrum to evaluate the effect of disorder on the operational bandwidth (Fig. 4). We observe that whereas both magnetic band states and CROW depend sensitively on the disorder (position/strength), from one realization to another, the edge states are insensitive to the specific parameters, as shown in the standard deviation of the reflectivity and delay time in Fig. 4a,b.

We note that, as time-reversal symmetry is not broken in our system, we cannot use such edge states as a one-way waveguide similar to ref. 50. More precisely, when we input a light field in the backward direction into the system (by swapping the input and output channel), the waveguides couple to the opposite rotating field in the resonators (opposite pseudo-spin) and experience a magnetic field with an opposite sign. Therefore, the system is reciprocal and the transport properties of the forward and backward feed are identical to each other.

We have also investigated the effect of loss in the resonators and other imperfections. Loss can be represented by a non-Hermitian term in the Hamiltonian: $-i\kappa_{in}\hat{a}_x^\dagger\hat{a}_x$, where κ_{in} characterizes propagation, bending and coupling losses (see Supplementary Information). The photonic loss attenuates the reflection in the edge state transfer band owing to the propagation around the perimeter (Fig. 4c). The effect of loss is similar in both 1D and 2D cases, and its magnitude is proportional to the number of resonators traversed by the light. Silicon-on-insulator technology, where more than 200 micro-ring resonators have been successfully coupled to each other[24], is a promising candidate for implementation of our scheme (see Supplementary Information for experimentally relevant parameters).

Other types of imperfection, such as surface roughness, can cause undesirable backscattering, which mixes pseudo-spin up and down, acting as 'magnetic disorder'. As shown in the Supplementary Information, these imperfections can be modelled by a magnetic disorder Hamiltonian. The backscattering effect manifests in the reduction of the signal in the R', T channels and some leakage in the R, T' channels. Figure 4c shows these transport coefficients. We observe that although the transport properties of 1D CROW and magnetic bands states are affected by such magnetic disorder, edge state transport remains robust, owing to the suppression of backscattering events. In particular, the scattering of a forward-going spin-up into a forward (backward)-going spin-down state is partially inhibited owing to an energy (momentum) mismatch.

Received 29 December 2010; accepted 8 July 2011; published online 21 August 2011

References

1. Klitzing, K. V. & Pepper, M. New method for high-accuracy determination of the fine-structure constant based on quantized Hall resistance. *Phys. Rev. Lett.* **45,** 494–497 (1980).
2. Tsui, D. C., Stormer, H. L. & Gossard, A. C. Two-dimensional magnetotransport in the extreme quantum limit. *Phys. Rev. Lett.* **48,** 1559–1562 (1982).
3. König, M. *et al.* Quantum spin Hall insulator state in HgTe quantum wells. *Science* **318,** 766–770 (2007).
4. Comtet, A., Jolicoeur, T., Ouvry, S. & David, F. (eds) *The Quantum Hall Effect: Novel Excitations and Broken Symmetries* (Spinger, 2000).
5. Prange, R. E., Girvin, S. M. & Cage, M. E. *The Quantum Hall Effect* (Springer, 1986).
6. Jeckelmann, B. & Jeanneret, B. The quantum Hall effect as an electrical resistance standard. *Rep. Prog. Phys.* **64,** 1603–1655 (2001).
7. Novoselov, K. *et al.* Room-temperature quantum Hall effect in graphene. *Science* **315,** 1379 (2007).
8. Kitaev, A. Fault-tolerant quantum computation by anyons. *Ann. Phys.* **303,** 2–30 (2003).
9. Nayak, C., Simon, S., Stern, A., Freedman, M. & Sarma, S. D. Fault-tolerant quantum computation by anyons. *Rev. Mod. Phys.* **80,** 1083–1159 (2008).
10. Cooper, N. Non-Abelian anyons and topological quantum computation. *Adv. Phys.* **57,** 539–616 (2008).
11. Haldane, F. & Raghu, S. Possible realization of directional optical waveguides in photonic crystals with broken time-reversal symmetry. *Phys. Rev. Lett.* **100,** 013904 (2008).
12. Cho, J., Angelakis, D. & Bose, S. Fractional quantum Hall state in coupled cavities. *Phys. Rev. Lett.* **101,** 246809 (2008).
13. Wang, Z., Chong, Y., Joannopoulos, J. & Soljačić, M. Reflection-free one-way edge modes in a gyromagnetic photonic crystal. *Phys. Rev. Lett.* **100,** 13905 (2008).
14. Otterbach, J., Ruseckas, J., Unanyan, R. G., Juzeliūnas, G. & Fleischhauer, M. Effective magnetic fields for stationary light. *Phys. Rev. Lett.* **104,** 033903 (2010).
15. Koch, J., Houck, A. A., Hur, K. L. & Girvin, S. M. Time-reversal symmetry breaking in circuit-QED based photon lattices. *Phys. Rev. A* **82,** 043811 (2010).
16. Kitagawa, T., Rudner, M., Berg, E. & Demler, E. Exploring topological phases with quantum walks. *Phys. Rev. A* **82,** 033429 (2010).
17. Azbel, M. Energy spectrum of a conduction electron in a magnetic field. *Sov. Phys. JETP* **19,** 634–649 (1964).
18. Kuhl, U. & Stöckmann, H. Microwave realization of the Hofstadter butterfly. *Phys. Rev. Lett.* **80,** 3232–3235 (1998).
19. Manela, O., Segev, M., Christodoulides, D. & Kip, D. Hofstadter butterflies in nonlinear Harper lattices, and their optical realizations. *New J. Phys.* **12,** 053017 (2010).
20. Haldane, F. Model for a quantum Hall effect without Landau levels: Condensed-matter realization of the 'parity anomaly'. *Phys. Rev. Lett.* **61,** 2015–2018 (1988).
21. Kane, C. & Mele, E. Quantum spin Hall effect in graphene. *Phys. Rev. Lett.* **95,** 226801 (2005).
22. Bernevig, B. & Zhang, S-C. Quantum spin Hall effect. *Phys. Rev. Lett.* **96,** 106802 (2006).
23. Xia, F., Sekaric, L. & Vlasov, Y. Ultracompact optical buffers on a silicon chip. *Nature Photon.* **1,** 65–71 (2007).
24. Cooper, M. L. *et al.* Statistics of light transport in 235-ring silicon coupled-resonator optical waveguides. *Opt. Express* **18,** 26505–26516 (2010).
25. Yariv, A., Xu, Y., Lee, R. & Scherer, A. Coupled-resonator optical waveguide: A proposal and analysis. *Opt. Lett.* **24,** 711–713 (1999).
26. Langbein, D. The tight-binding and the nearly-free-electron approach to lattice electrons in external magnetic fields. *Phys. Rev.* **180,** 633–648 (1969).
27. Hofstadter, D. Energy levels and wave functions of Bloch electrons in rational and irrational magnetic fields. *Phys. Rev. B* **14,** 2239–2249 (1976).
28. Gardiner, C. W. & Collett, M. J. Input and output in damped quantum systems: Quantum stochastic differential equations and the master equation. *Phys. Rev. A* **31,** 3761–3774 (1985).
29. Heebner, J. *et al.* Enhanced linear and nonlinear optical phase response of AlGaAs microring resonators. *Opt. Lett.* **29,** 769–771 (2004).
30. Xia, F., Sekaric, L. & Vlasov, Y. Mode conversion losses in silicon-on-insulator photonic wire based racetrack resonators. *Opt. Express* **14,** 3872–3886 (2006).
31. Bychkov, Y. & Rashba, E. Oscillatory effects and the magnetic susceptibility of carriers in inversion layers. *J. Phys. C* **17,** 6039–6045 (1984).
32. Fan, S. *et al.* Theoretical analysis of channel drop tunneling processes. *Phys. Rev. B* **59,** 15882–15892 (1999).
33. Xu, Y., Li, Y., Lee, R. & Yariv, A. Scattering-theory analysis of waveguide-resonator coupling. *Phys. Rev. E* **62,** 7389–7404 (2000).
34. Halperin, B. Quantized Hall conductance, current-carrying edge states, and the existence of extended states in a two-dimensional disordered potential. *Phys. Rev. B* **25,** 2185–2190 (1982).
35. Rammal, R., Toulouse, G., Jaekel, M. & Halperin, B. Quantized Hall conductance and edge states: Two-dimensional strips with a periodic potential. *Phys. Rev. B* **27,** 5142–5145 (1983).
36. Hatsugai, Y. Edge states in the integer quantum Hall effect and the Riemann surface of the Bloch function. *Phys. Rev. B* **48,** 11851–11862 (1993).
37. Barwicz, T. *et al.* Fabrication of add-drop filters based on frequency-matched microring resonators. *J. Lightwave Technol.* **24,** 2207–2218 (2006).
38. Ferrari, C., Morichetti, F. & Melloni, A. Disorder in coupled-resonator optical waveguides. *J. Opt. Soc. Am. B* **26,** 858–866 (2009).
39. Anderson, P. W. Absence of diffusion in certain random lattices. *Phys. Rev.* **109,** 1492–1505 (1958).
40. Kramer, B. & Mackinnon, A. Localization: Theory and experiment. *Rep. Prog. Phys.* **56,** 1469–1564 (1993).
41. Mookherjea, S., Park, J. S., Yang, S-H. & Bandaru, P. R. Localization in silicon nanophotonic slow-light waveguides. *Nature Photon.* **2,** 90–93 (2008).
42. Lahini, Y. *et al.* Anderson localization and nonlinearity in one-dimensional disordered photonic lattices. *Phys. Rev. Lett.* **100,** 013906 (2008).
43. Thouless, D. J., Kohmoto, M., Nightingale, M. P. & den Nijs, M. Quantized Hall conductance in a two-dimensional periodic potential. *Phys. Rev. Lett.* **49,** 405–408 (1982).
44. Schwartz, T., Bartal, G., Fishman, S. & Segev, M. Transport and Anderson localization in disordered two-dimensional photonic lattices. *Nature* **446,** 52–55 (2007).
45. Baba, T Slow light in photonic crystals. *Nature Photon.* **2,** 465–473 (2008).
46. Huckestein, B. Scaling theory of the integer quantum Hall effect. *Rev. Mod. Phys.* **67,** 357–396 (1995).
47. Lahini, Y., Bromberg, Y., Christodoulides, D. & Silberberg, Y. Quantum correlations in two-particle Anderson localization. *Phys. Rev. Lett.* **105,** 163905 (2010).
48. Srinivasan, K. & Painter, O. Linear and nonlinear optical spectroscopy of a strongly coupled microdisk-quantum dot system. *Nature* **450,** 862–866 (2007).
49. Hafezi, M., Chang, D. E., Gritsev, V., Demler, E. & Lukin, M. D. Photonic quantum transport in a nonlinear optical fiber. *Europhys. Lett.* **94,** 54006 (2011).
50. Wang, Z., Chong, Y., Joannopoulos, J. D. & Soljacic, M. Observation of unidirectional backscattering-immune topological electromagnetic states. *Nature* **461,** 772–776 (2009).

Acknowledgements

The authors wish to thank G. Solomon, E. Waks, S. Fan and B. Halperin for helpful discussions. This research was supported by the US Army Research Office MURI award W911NF0910406, NSF, AFOSR Quantum Simulation MURI, ARO-MURI on Atomtronics, Packard, DARPA QUEST, DARPA OLE and Harvard-MIT CUA.

Author contributions

M.H., E.A.D., M.D.L. and J.M.T. contributed to the conceptual development of the project and editing of the manuscript. M.H. carried out the mathematical analysis and simulations and wrote the manuscript.

Additional information

The authors declare no competing financial interests. Supplementary information accompanies this paper on www.nature.com/naturephysics. Reprints and permissions information is available online at http://www.nature.com/reprints. Correspondence and requests for materials should be addressed to M.H.